ACS Medicinal Chemistry Letters

pubs.acs.org/acsmedchemlett

Letter

Exploration of a 14-3-3 PPI Pocket by Covalent Fragments as Stabilizers

Eline Sijbesma, Kenneth K. Hallenbeck, Sebastian A. Andrei, Reanne R. Rust, Joris M. C. Adriaans, Luc Brunsveld,* Michelle R. Arkin,* and Christian Ottmann*

Cite This: ACS Med. Chem. Lett. 2021, 12, 976–982

Read Online

ACCESS | Metrics & More | Article Recommendations | Supporting Information

ABSTRACT: The systematic discovery of functional fragments binding to the composite interface of protein complexes is a first critical step for the development of orthosteric stabilizers of protein−protein interactions (PPIs). We have previously shown that disulfide trapping successfully yielded covalent stabilizers for the PPI of 14-3-3 with the estrogen receptor ERα. Here we provide an assessment of the composite PPI target pocket and the molecular characteristics of various fragments binding to a specific subpocket. Evaluating structure−activity relationships highlights the basic principles for PPI stabilization by these covalent fragments that engage a relatively large and exposed binding pocket at the protein/peptide interface with a "molecular glue" mode of action.

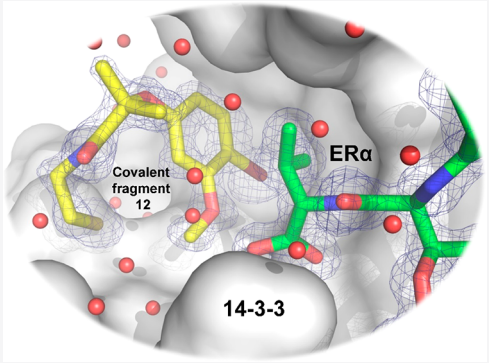

KEYWORDS: *Protein−protein interactions, PPI stabilization, fragment-based drug discovery, covalent binder*

The modulation of protein−protein interactions (PPIs) by small molecule ligands is a highly sought-after strategy for chemical biology and drug discovery.[1−4] PPI stabilization and inhibition are related approaches but based on profoundly different underlying principles.[5,6] The stabilization of protein complexes by cooperatively binding ligands could have tremendous benefit in terms of client selectivity since druggable pockets at binding interfaces are constituted of residues of both protein partners and thus only exist in the context of the complex.[2,7,8] In contrast, PPI inhibitors typically affect multiple interactions of the target protein, an important consideration when aiming to therapeutically target interactions of "hub" proteins that have a large number of binding partners.[9−11] However, strategies to systematically screen for small-molecule stabilizers are scarce. Since our interest focuses on the interactions of the hub protein 14-3-3, we set out to develop innovative strategies to discover new cooperative ligands as stabilizers for 14-3-3 PPIs. The 14-3-3 proteins regulate a number of important disease-related proteins; in many cases, stabilization of the 14-3-3/client complex is predicted to have a therapeutic effect.[12−24] For instance, binding of 14-3-3 to the C-terminus of estrogen receptor (ERα) phosphorylated at T594 inhibits ERα activity; stabilization of the interaction by the natural product fusicoccin-A (FC-A) blocks growth of ERα-dependent cells.[22] Hence, small molecule 14-3-3 PPI stabilizers could be useful chemical probes or starting points for drug discovery.

We have previously presented a site-directed fragment-based screening approach (disulfide trapping), by which we successfully selected fragments that enhanced the affinity between 14-3-3 and ERα.[25] We incubated the cysteine-containing 14-3-3 protein with a disulfide library in the presence or absence of ERα-derived phosphopeptide (ERα-pp) and analyzed conjugate formation by intact-protein mass spectrometry. The most effective covalent stabilizers increased the PPI complex affinity by 40-fold. The molecular mechanism was elucidated by X-ray cocrystal structures which revealed a "molecular glue" mode of action, whereby the fragment efficiently engaged a subpocket at the composite PPI interface, interacting with both partners.

Here, we present the results of a study into the properties of disulfide-tethered ligands and analyze both the affinity of fragments at the 14-3-3 PPI pocket and the cooperativity observed for fragments engaging a specific subpocket. The position of the cysteine residue used for screening by disulfide trapping was found to be crucial. Comparing covalent fragments tethered to different engineered cysteine residues along the rim of the pocket provided insight into pocket ligandability by fragments. Residue C42 was suitable for finding stabilizing fragments, whereas fragments bound to a

Received: February 9, 2021
Accepted: May 4, 2021
Published: May 10, 2021

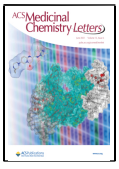

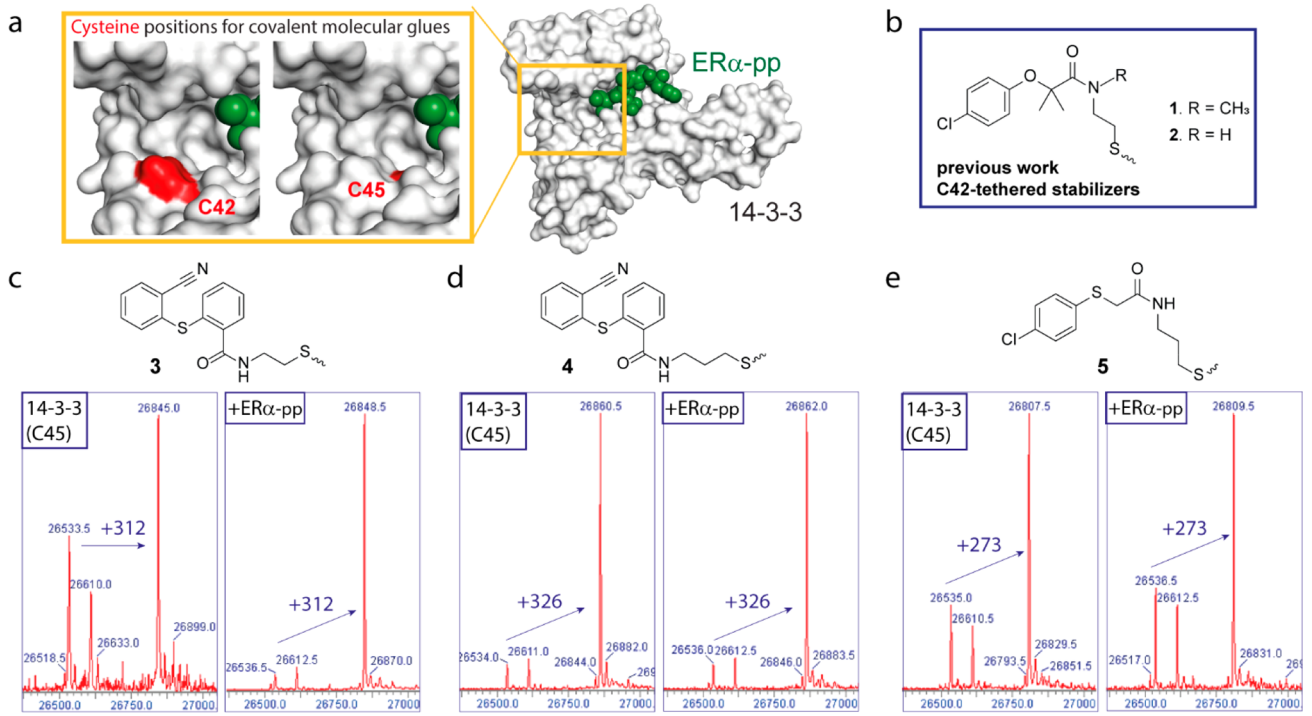

Figure 1. Disulfide trapping identify ligands for 14-3-3σ. (a) Target pocket for the site-directed disulfide-trapping approach, highlighting two cysteine mutations (C42, C45; red surface areas) in the 14-3-3σ (white surface)/ERα-pp (green spheres) pocket. (b) Chemical structures of previously described 14-3-3σ/ERα-pp stabilizers **1** and **2**.[25] (c–e) Chemical structures and disulfide trapping screening results for C45 hits. Mass spectra for 14-3-3σ(C45) conjugated to fragment **3** (c), **4** (d), and **5** (e) in the absence (left) or presence (right) of ERα-pp. The adduct shift between *apo* protein [expected mass 26 536 Da, 2-mercaptoethanol (βME)-capped mass 26 612 Da] and protein-disulfide conjugate mass is indicated with arrows. Conditions for mass spectrometry: 100 nM 14-3-3σ, 200 nM ERα-pp, 100 μM fragment, 100 μM βME.

greater extent, but not cooperatively, to a cysteine at position 45 (C45). Both sites yielded several X-ray cocrystal structures that provided hypotheses for binding affinity and cooperativity. Even though these cysteine positions are non-native to 14-3-3 isoforms and optimization of fragments toward noncovalent stabilizers represents a next challenge, initial structure–activity relationships (SARs) were explored for the main cooperative hit tethered to 14-3-3σ(C42), aiding our understanding of the rules for 14-3-3/client stabilization by covalent fragments.

Covalent Fragments Tethered to 14-3-3σ C45. Covalent fragments that strongly stabilized the interaction between 14-3-3 and ERα were described previously.[25] Briefly, in a site-directed screening approach, we varied the position of a cysteine residue serving as a reactive handle for thiol–disulfide exchange with a library of ~1600 disulfide-containing fragments. We introduced cysteines at residues 42 and 45 on 14-3-3σ at the base of the target pocket adjacent to the C-terminus of the ERα-pp in the protein/peptide complex (Figure 1a). Fragments **1** and **2**, tethered to 14-3-3σ(C42), showed the best stabilization of the 14-3-3/ERα-pp complex (Figure 1b; for which intact mass spectrometry (MS), fluorescence polarization (FP), and X-ray crystallography data was presented previously[25]); however, we also identified fragments tethered to 14-3-3σ(C45). MS data of three hits are presented here (Figure 1c–e). Of these, fragment **3** was ~50% bound to 14-3-3σ(C45) in the absence of ERα-pp and ~90% bound to 14-3-3σ(C45) in the presence of ERα-pp, based on intact mass spectrometry (MS; Figure 1c). Additional fragments displayed high % bound, as observed from the protein-conjugate peaks for **4** and **5** (Figure 1d,e). Here, no difference was observed between 14 and 3–3σ(C45) *apo* or ERα-pp bound, indicating a strong affinity of these fragments to 14-3-3 alone and no additional influence from the ERα peptide on fragment binding. There is thus no initial indication of PPI stabilizing or inhibiting activity.

Soaking cocrystals of 14-3-3σ(C45)/ERα-pp enabled the observation of electron density for the three fragments **3**–**5**, with the most convincing, continuous density for **3** (Figure 2a). **4** only differs from **3** by the addition of a longer alkyl chain (C3 versus C2 in **3**), resulting in a less optimal binding pose in the PPI complex (Figure 2b). Fragment **5** features a chlorophenyl moiety, as is seen in fragments **1** and **2** (Figure 2c);[25] interestingly, while the Cl moiety is positioned identically, the phenyl ring of **5** is slightly tilted relative to **2** (Figure 2d). To determine whether fragments **3**–**5** stabilized the 14-3-3σ(C45)/ERα-pp complex, we measured the binding of fluorescein-labeled ERα-pp to 14-3-3σ(C45) by fluorescence anisotropy. Notably, fragments **3**–**5** did not induce 14-3-3σ(C45)/ERα-pp complex formation, implying no stabilization of the protein/peptide complex (Figure S1). This observation was particularly striking for **3**, given the close proximity between the fragment and ERα-pp in the X-ray cocrystal structure (Figure 2a), and its apparent increased binding to 14-3-3σ(C45) in the presence of ERα-pp observed by mass spectrometry (Figure 1c).

The lack of cooperativity for fragments **3**–**5** was confirmed in MS titration experiments, performed under stronger reducing conditions (1 mM βME) emphasizing the noncovalent contribution of the fragment in stabilizing the PPI. Here, the conjugation peak for 14-3-3σ(C45)-**3** indicated >80% tethering for all concentrations of fragment **3** (100 nM to 1 mM), which was not influenced by the presence of ERα-

https://doi.org/10.1021/acsmedchemlett.1c00088
ACS Med. Chem. Lett. 2021, 12, 976–982

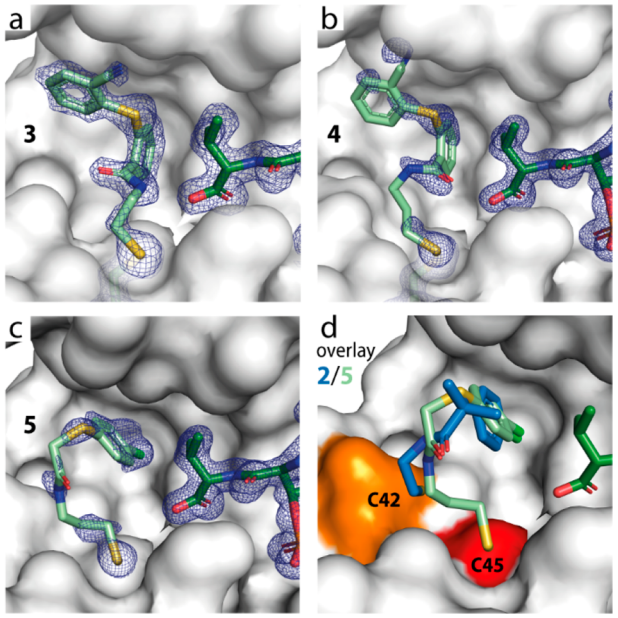

Figure 2. Close-up views of the binding pocket for cocrystal structures of 14-3-3σ(C45)-tethered fragment **3**−**5** (a−c, mint sticks). $2F_o$-F_c electron density maps are contoured at 1σ, 14-3-3σ is shown as white surface, and ERα-pp as dark green sticks. (d) Crystallographic overlay for C42-bound fragment **2** (blue) and C45-bound **5** (mint).

pp under these conditions (Figure 3a). Interestingly, a dose−response effect was observed for titration of **3** to 14-3-3σ(C42), where the presence of ERα-pp slightly increased %-tethering at all concentrations (Figure 3b). In contrast, fragment **1** showed cooperative tethering to both cysteine positions, with the larger effect observed for C42 (Figure 3c,d). Whereas **3** for C45 tethered similarly over the entire concentration range, fragment **1** showed a steep S-curve and only reached >80% tethering at high concentrations. The cooperative difference for **3** tethered to C42 versus C45 was further confirmed by fluorescence anisotropy, where fluorescein-labeled ERα-pp binding was enhanced upon titration of 14-3-3σ(C42) with **3** (EC_{50} 0.9 ± 0.11 μM, Figure 3c). These results indicated that, in addition to the appropriate chemophore, the covalent tethering position was also important to elicit stabilization. Together, these data suggested that even though the C45-tethered fragments bound tightly to the 14-3-3 pocket, they lacked significant stabilizing activity toward the motif, suggesting that the disulfide bond formation between **3** and 14-3-3 C45 contributed a degree of cooperativity observed in the primary screen. Since they also did not show any inhibition toward the PPI under study, these fragments, as neutral binders, were compatible with the binary complex but did not engage the composite interface enough to drive orthosteric cooperativity. Thus, cooperativity in PPI binding is finely tuned and depends on an optimal positioning of all molecular elements.[26,27]

These results illustrate that strong binding of a fragment to the PPI complex does not necessarily result in PPI stabilizing activity. Indeed, when looking in more detail at data for C42 hits, strong tethering by itself or clear density in a cocrystal structure are not per se good predictors of stabilizing activity toward 14-3-3/ERα-pp, whereas differential dose−response behavior of tethered fragments in absence or presence of ERα-pp by MS is nicely correlated with stabilization in fluorescence anisotropy. Fragment **1** displayed high % tethering to 14-3-3σ(C42) only in the presence of ERα-pp, where >80% tethering is observed for all concentrations of fragment **1** (Figure 3d), which is reflected by efficient stabilization of 14-3-3/ERα-pp by **1**.[25] The X-ray cocrystal structures display similarly clear density for fragments **1** and **3**, further confirming that a good binder (even to a composite pocket) is not sufficient nor necessarily predictive of PPI stabilization

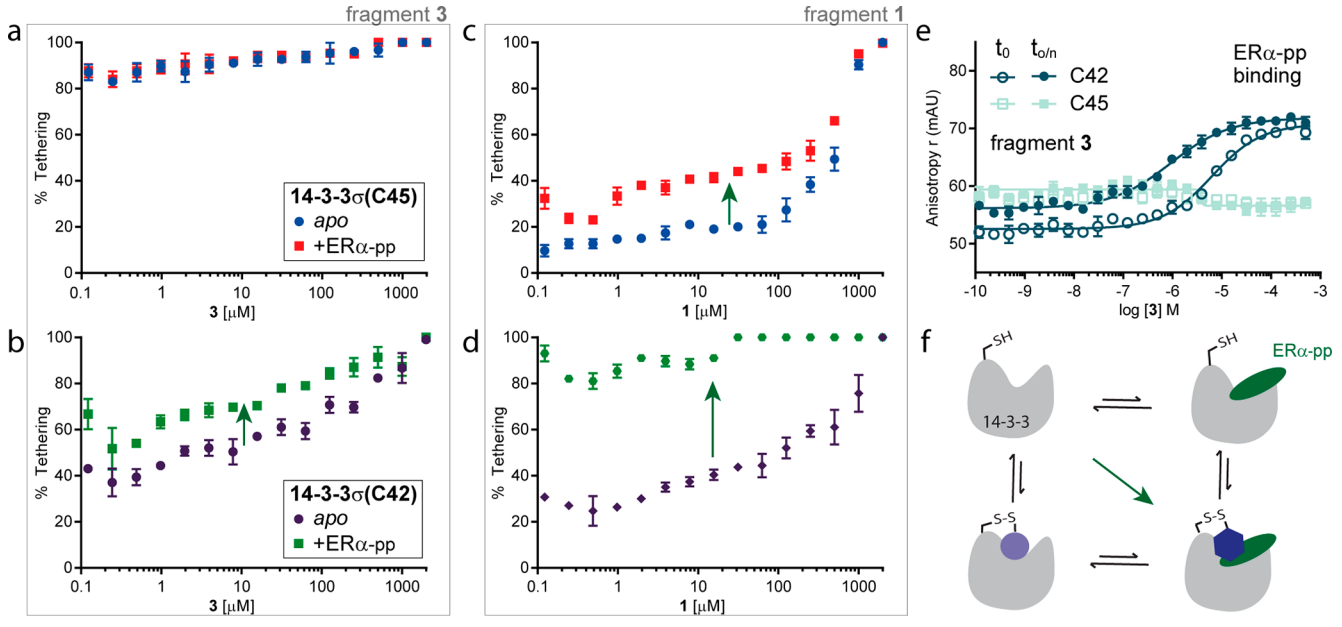

Figure 3. Analysis of cooperative binding to 14-3-3σ of tethered fragments with ERα-pp. Dose−response data of protein−fragment conjugate formation for 14-3-3σ C45 (a and c) or C42 (b and d), titrated with fragment **3** or **1**, respectively, and analyzed by intact-protein mass spectrometry (MS). 100 nM 14-3-3σ, 200 nM ERα-pp, 100 μM fragment, 1 mM βME. (e) Fluorescence anisotropy dose−response curves for 14-3-3σ(C45 or C42) and fluorescein-labeled ERα-pp titrated with fragment **3**. Data for time point 0 (t_0) and at end point (after overnight incubation, $t_{o/n}$) are displayed. (f) Schematic illustration of binding equilibria for ternary complex formation.

https://doi.org/10.1021/acsmedchemlett.1c00088
ACS Med. Chem. Lett. 2021, 12, 976−982

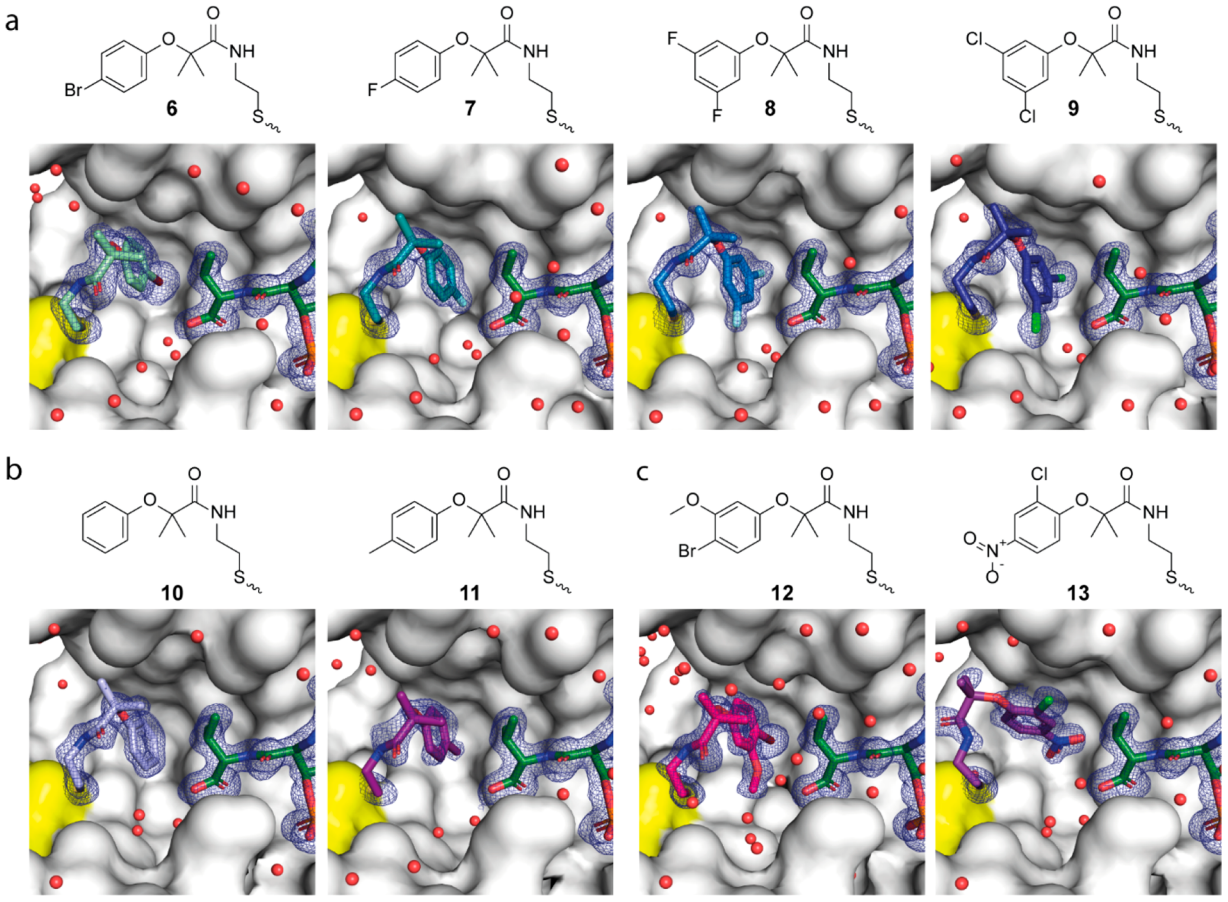

Figure 4. Derivatives of 14-3-3σ(C42)/ERα-pp stabilizer **2**. Chemical structures and X-ray cocrystal structures of compounds **6**–**13** in the binding pocket tethered to C42 (yellow surface). $2F_o$-F_c electron density maps are contoured at 1σ. Water molecules are depicted as red spheres.

potential. Furthermore, the data suggest that the C45 position of 14-3-3 does not allow the fragments in our library to achieve the proper orientation to stabilize the 14-3-3σ/ERα-pp complex.

Derivatives of 14-3-3 C42-Tethered Stabilizers. A small library of derivatives of fragment **2** was then synthesized to assess the main contributing factors to the 14-3-3/ERα-pp stabilizing activity. X-ray cocrystal structures were obtained for eight disulfide fragments tethered to 14-3-3σ(C42) bound by ERα-pp (Figure 4). The most resolved electron density was observed for variants with a single *para*- or double *meta*-halogen substituent on the phenyl (**6**–**9**, Figure 4a). An unsubstituted phenyl (**10**) and a *p*-methylphenyl (**11**) showed weaker electron density (Figure 4b). An *m*-methoxy in addition to a *p*-bromo substituent resulted in well-resolved electron density for **12**, whereas a combination of *o*-chloro and *p*-nitro substituents was less beneficial, resulting in electron density mainly for the phenyl group and only part of the linker for **13** (Figure 4c). Compared to the rest of the series, the phenyl ring of **13** was also rotated by 90°, directed by the *o*-chloro and resulting in the subsequent relocation of the linker.

Crystallographic overlays of compounds **6**–**12** with **2** (PDB entry 6HMT)[25] reveals the apparent strict positioning of the halogen in the pocket, specifically when comparing single substituents on the para-position to double meta-substituents (Figure 5a,b). For the double meta-substituted compounds, the molecules are reorientated so that one of the halogens (in **8** and **9**) overlays with the *para*-chloro position of **2**. The unsubstituted or *p*-fluorophenyl are less directing (Figure 5c), while a *p*-methyl or the *p*-bromo/*m*-methoxy combination perfectly overlays with the position of **2** (Figure 5d). While all

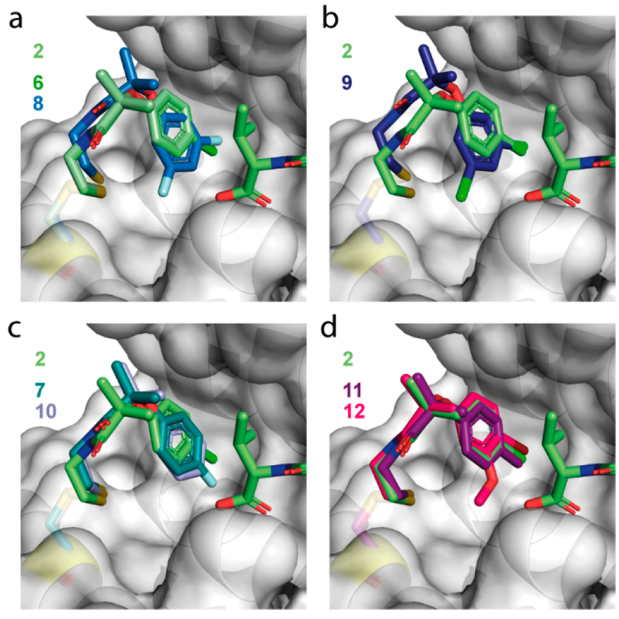

Figure 5. Crystallographic overlays for **6**–**12**. Fragments tethered to 14-3-3σ(C42) bound by ERα-pp, overlaid on the X-ray cocrystal structure of the original stabilizer **2** (PDB entry 6HMT).

https://doi.org/10.1021/acsmedchemlett.1c00088
ACS Med. Chem. Lett. 2021, 12, 976–982

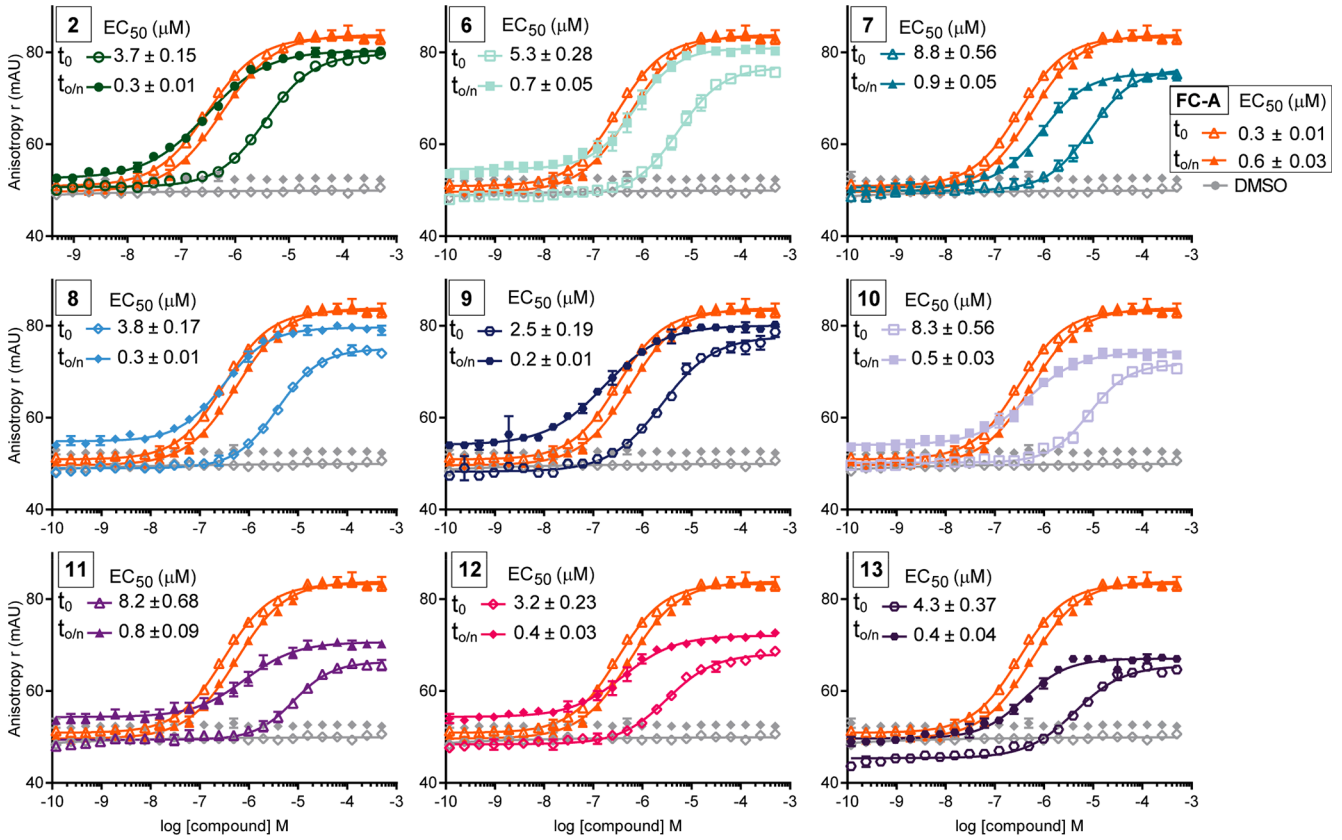

Figure 6. Stabilization activity for a focused library of fragment **2** structure variations. Dose−response curves of 14-3-3σ(C42) and fluorescein-labeled ERα-pp titrated with FC-A (orange), **2**, and **6**−**13**. Fluorescence anisotropy data and corresponding EC_{50} values, at time point 0 (t_0) and at end point (after overnight incubation, $t_{o/n}$) are displayed.

compounds occupy this same subpocket, **13** shows the most divergent binding pose (Figure S2a).

A potential stabilization activity of **6**−**13** was analyzed in fluorescence anisotropy experiments by titrating 14-3-3σ(C42) and ERα-pp with the fragments (Figure 6). Data were collected directly after preparing the samples (t_0) and after reaching equilibrium (at end point, after overnight incubation, $t_{o/n}$). All derivatives were found to be stabilizers of the 14-3-3σ/ERα-pp complex as indicated by enhanced ERα-pp binding upon fragment titrations, displaying EC_{50} values (173−911 nM) in the same range as **2** (EC_{50} 299 ± 14 nM). Whereas the equilibrium was near-instantaneous for stabilization by the natural product FC-A, PPI stabilization induced by tethered fragments binding upon thiol−disulfide exchange logically displayed slower kinetics, perhaps due to the absence of βME in these experiments. The $t_{o/n}$ curve was shifted to the left, resulting in roughly 10-fold improved EC_{50} values compared to t_0. Additionally, upper plateaus for **6**, **8**, and **9** reached anisotropy values similar to FC-A and **2**, while for **7**, **10**, and **11**−**13** the maximum anisotropy was lower, possibly caused by a reduced stabilization of the distal region of ERα-pp. This was reflected in the X-ray cocrystal structures, where the side chain of the phenylalanine at the −2 position (F591) was flexible, revealing different orientations and in two cocrystal structures; additional density was also observed for G590 (Figure S2b).

This small set of derivatives is not sufficient for the establishment of a complete SAR, yet it does provide several valuable insights. First, it is interesting to find that all variations are tolerated and only influence stabilization activity within a 3-fold range of EC_{50} values. Second, a halogen on the phenyl is highly beneficial for orientation into the identified subpocket, as the strongest stabilization and most resolved electron density are observed for both *p*-chloro (**2**) and *p*-bromo (**6**) and doubly substituted *m,m*-fluoro (**8**) and *m,m*-chloro- (**9**) phenyls. Finally, the constraining effect of the dimethyl moiety on the linker appears important for achieving a specific orientation. The surface complementarity of the fragments' binding site, constituted jointly by the protein/peptide, further explains the differences between C42/C45-binding fragments. The binding pocket of 14-3-3/ERα is defined by several molecular recognition elements, most optimally engaged by the potent stabilizer and tool-compound FC-A (Figure S3a). The part of the pocket toward the peptide C-terminus is defined by a hydrophobic patch shaped by the "roof-of-the-groove" 14-3-3 residues L218, I219, and L222 and V595 of ERα. The C42-tethered fragments show optimal orientation of a dimethyl moiety and of the phenyl-halogen facing toward V595, thereby nestling in that hydrophobic patch in a shape-complementary fashion, resulting in a stabilizing effect toward the peptide binding (Figure S3b). In comparison, C45 binders are tethered to the protein in too close proximity to the peptide. Even though strong binding is observed to the protein by itself, the majority of the noncovalent contributions are directed toward the 14-3-3 protein pocket pointing away from the peptide. Additionally, two 14-3-3 lysine residues at the base of the groove close to the peptide C-terminus, K122 and K49, hydrogen-bond to FC-A. Finally, an important feature of FC-A stabilization of the 14-3-3/ERα complex is the hydrogen bonding network between two FC-A hydroxyl groups and 14-3-3's D215, which is pulled toward the compound, thereby

https://doi.org/10.1021/acsmedchemlett.1c00088
ACS Med. Chem. Lett. 2021, 12, 976−982

dragging helix 9 down toward the binding pocket (Figure S3a). We have reported previously that this interaction is crucial for a potent stabilizing allosteric effect.[28] Whereas this residue is engaged by neither C42/C45 binders reported here, it constitutes an interesting opportunity for future optimization of tethered fragments toward potent (noncovalent) 14-3-3 PPI stabilizers.

In this work, we described covalent fragments that bound to two engineered cysteine residues near the pocket formed by the 14-3-3σ/ERα-pp complex. These fragments were identified via disulfide trapping ("tethering") screens that we proposed as a systematic strategy for the discovery of PPI stabilizers. Cooperative stabilization was achieved via tethering to C42, whereas tethering to C45 resulted in neutral binders based on similar chemophores. X-ray cocrystal structures combined with biochemical binding studies revealed that tight binding alone did not necessarily guarantee effective PPI stabilization. C42 appeared to be ideally located for identifying optimal stabilizers for 14-3-3/ERα from this disulfide library. Some fragments, particularly tethered to C45, strongly bound to 14-3-3 without influencing ERα binding. Coupled with an understanding of the features that lead to PPI stabilization, these tightly bound compounds could perhaps be chemical optimized into effective stabilizers. The ability to optimize screening for local differences in target pockets is an important benefit of a reversible covalent-fragment screening strategy and further illustrates the suitability of the tethering approach to identify stabilizers for adaptive interfaces and composite PPI pockets.

■ ASSOCIATED CONTENT

Supporting Information

The Supporting Information is available free of charge at https://pubs.acs.org/doi/10.1021/acsmedchemlett.1c00088.

Experimental procedures; fluorescence anisotropy dose−response curves; crystallographic overlays; binding modes of FC-A and C42- and C45-tethered fragments; XRD data collection and refinement statistics; ^{13}C NMR and ^{1}H NMR spectra (PDF)

■ AUTHOR INFORMATION

Corresponding Authors

Luc Brunsveld − *Laboratory of Chemical Biology, Department of Biomedical Engineering and Institute for Complex Molecular Systems (ICMS), Eindhoven University of Technology, 5600 MB Eindhoven, The Netherlands;* orcid.org/0000-0001-5675-511X; Email: l.brunsveld@tue.nl

Michelle R. Arkin − *Department of Pharmaceutical Chemistry and Small Molecule Discovery Center (SMDC), University of California, San Francisco 94134, United States;* orcid.org/0000-0002-9366-6770; Email: michelle.arkin@ucsf.edu

Christian Ottmann − *Laboratory of Chemical Biology, Department of Biomedical Engineering and Institute for Complex Molecular Systems (ICMS), Eindhoven University of Technology, 5600 MB Eindhoven, The Netherlands;* orcid.org/0000-0001-7315-0315; Email: c.ottmann@tue.nl

Authors

Eline Sijbesma − *Laboratory of Chemical Biology, Department of Biomedical Engineering and Institute for Complex Molecular Systems (ICMS), Eindhoven University of Technology, 5600 MB Eindhoven, The Netherlands*

Kenneth K. Hallenbeck − *Department of Pharmaceutical Chemistry and Small Molecule Discovery Center (SMDC), University of California, San Francisco 94134, United States*

Sebastian A. Andrei − *Laboratory of Chemical Biology, Department of Biomedical Engineering and Institute for Complex Molecular Systems (ICMS), Eindhoven University of Technology, 5600 MB Eindhoven, The Netherlands*

Reanne R. Rust − *Laboratory of Chemical Biology, Department of Biomedical Engineering and Institute for Complex Molecular Systems (ICMS), Eindhoven University of Technology, 5600 MB Eindhoven, The Netherlands*

Joris M. C. Adriaans − *Laboratory of Chemical Biology, Department of Biomedical Engineering and Institute for Complex Molecular Systems (ICMS), Eindhoven University of Technology, 5600 MB Eindhoven, The Netherlands*

Complete contact information is available at: https://pubs.acs.org/10.1021/acsmedchemlett.1c00088

Author Contributions

The manuscript was written through contributions of all authors. All authors have given approval to the final version of the manuscript.

Funding

This research was supported by The Netherlands Organization for Scientific Research (through Gravity Program 024.001.035, VICI grant 016.150.366 and ECHO grant 711.018.003).

Notes

The authors declare the following competing financial interest(s): E.S. is full-time employee of Ambagon Therapeutics, L.B., M.R.A., and C.O. are founders and shareholders of Ambagon Therapeutics.

Crystallographic structure data were deposited in the Protein Data Bank (PDB) and obtained IDs: 7B9M, 7B9R, 7B9T, 7BA3, 7BA5, 7BA6, 7BA7, 7BA8, 7BA9, 7BAA, and 7BAB.

■ ACKNOWLEDGMENTS

We acknowledge the Renslo laboratory for synthesis of the SMDC disulfide library and thank J. Schill for assistance with synthesis and characterization.

■ ABBREVIATIONS

PPI, protein−protein interaction; SAR, structure−activity relationship; ERα, estrogen receptor alpha; FC-A, fusicoccin-A; pp, phosphopeptide; MS, mass spectrometry; βME, 2-mercaptoethanol; FA, fluorescence anisotropy.

■ REFERENCES

(1) Arkin, M. R.; Tang, Y.; Wells, J. A. Small-Molecule Inhibitors of Protein-Protein Interactions: Progressing toward the Reality. *Chem. Biol.* **2014**, *21* (9), 1102−1114.

(2) Petta, I.; Lievens, S.; Libert, C.; Tavernier, J.; De Bosscher, K. Modulation of Protein-Protein Interactions for the Development of Novel Therapeutics. *Mol. Ther.* **2016**, *24* (4), 707−718.

(3) Wells, J. A.; McClendon, C. L. Reaching for High-Hanging Fruit in Drug Discovery at Protein-Protein Interfaces. *Nature* **2007**, *450* (7172), 1001−1009.

(4) Milroy, L.-G.; Grossmann, T. N.; Hennig, S.; Brunsveld, L.; Ottmann, C. Modulators of Protein-Protein Interactions. *Chem. Rev.* **2014**, *114* (9), 4695−4748.

(5) Zarzycka, B.; Kuenemann, M. A.; Miteva, M. A.; Nicolaes, G. A. F.; Vriend, G.; Sperandio, O. Stabilization of Protein−Protein

Interaction Complexes through Small Molecules. *Drug Discovery Today* **2016**, *21* (1), 48−57.
(6) Fischer, G.; Rossmann, M.; Hyvönen, M. Alternative Modulation of Protein-Protein Interactions by Small Molecules. *Curr. Opin. Biotechnol.* **2015**, *35*, 78−85.
(7) Andrei, S. A.; Sijbesma, E.; Hann, M.; Davis, J.; O'Mahony, G.; Perry, M. W. D.; Karawajczyk, A.; Eickhoff, J.; Brunsveld, L.; Doveston, R. G.; Milroy, L.-G.; Ottmann, C. Stabilization of Protein-Protein Interactions in Drug Discovery. *Expert Opin. Drug Discovery* **2017**, *12* (9), 925−940.
(8) de Vink, P. J.; Andrei, S. A.; Higuchi, Y.; Ottmann, C.; Milroy, L.-G.; Brunsveld, L. Cooperativity Basis for Small-Molecule Stabilization of Protein−Protein Interactions. *Chem. Sci.* **2019**, *10* (10), 2869−2874.
(9) Hartwell, L. H.; Hopfield, J. J.; Leibler, S.; Murray, A. W. From Molecular to Modular Cell Biology. *Nature* **1999**, *402* (S6761), C47−C52.
(10) Han, J.-D. J.; Bertin, N.; Hao, T.; Goldberg, D. S.; Berriz, G. F.; Zhang, L. V.; Dupuy, D.; Walhout, A. J. M.; Cusick, M. E.; Roth, F. P.; Vidal, M. Evidence for Dynamically Organized Modularity in the Yeast Protein−Protein Interaction Network. *Nature* **2004**, *430* (6995), 88−93.
(11) Jeong, H.; Mason, S. P.; Barabási, A.-L.; Oltvai, Z. N. Lethality and Centrality in Protein Networks. *Nature* **2001**, *411* (6833), 41−42.
(12) Rajagopalan, S.; Jaulent, A. M.; Wells, M.; Veprintsev, D. B.; Fersht, A. R. 14−3-3 Activation of DNA Binding of P53 by Enhancing Its Association into Tetramers. *Nucleic Acids Res.* **2008**, *36* (18), 5983−5991.
(13) Schumacher, B.; Mondry, J.; Thiel, P.; Weyand, M.; Ottmann, C. Structure of the P53 C-Terminus Bound to 14−3-3: Implications for Stabilization of the P53 Tetramer. *FEBS Lett.* **2010**, *584* (8), 1443−1448.
(14) Kuusk, A.; Neves, J. F.; Bravo-Rodriguez, K.; Gunnarsson, A.; Ruiz-Blanco, Y. B.; Ehrmann, M.; Chen, H.; Landrieu, I.; Sanchez-Garcia, E.; Boyd, H.; Ottmann, C.; Doveston, R. G. Adoption of a Turn Conformation Drives the Binding Affinity of P53 C-Terminal Domain Peptides to 14−3-3σ. *ACS Chem. Biol.* **2020**, *15* (1), 262−271.
(15) Molzan, M.; Ottmann, C. Synergistic Binding of the Phosphorylated S233- and S259-Binding Sites of C-RAF to One 14−3-3ζ Dimer. *J. Mol. Biol.* **2012**, *423* (4), 486−495.
(16) Kondo, Y.; Ognjenović, J.; Banerjee, S.; Karandur, D.; Merk, A.; Kulhanek, K.; Wong, K.; Roose, J. P.; Subramaniam, S.; Kuriyan, J. Cryo-EM Structure of a Dimeric B-Raf:14−3-3 Complex Reveals Asymmetry in the Active Sites of B-Raf Kinases. *Science* **2019**, *366* (6461), 109−115.
(17) Park, E.; Rawson, S.; Li, K.; Kim, B.-W.; Ficarro, S. B.; Pino, G. G.-D.; Sharif, H.; Marto, J. A.; Jeon, H.; Eck, M. J. Architecture of Autoinhibited and Active BRAF−MEK1−14−3-3 Complexes. *Nature* **2019**, *575* (7783), 545−550.
(18) Saha, M.; Carriere, A.; Cheerathodi, M.; Zhang, X.; Lavoie, G.; Rush, J.; Roux, P. P.; Ballif, B. A. RSK Phosphorylates SOS1 Creating 14−3-3 Docking Sites and Negatively Regulating MAPK Activation. *Biochem. J.* **2012**, *447* (1), 159−166.
(19) Ballone, A.; Centorrino, F.; Wolter, M.; Ottmann, C. Structural Characterization of 14−3-3ζ in Complex with the Human Son of Sevenless Homolog 1 (SOS1). *J. Struct. Biol.* **2018**, *202* (3), 210−215.
(20) Reincke, M.; Sbiera, S.; Hayakawa, A.; Theodoropoulou, M.; Osswald, A.; Beuschlein, F.; Meitinger, T.; Mizuno-Yamasaki, E.; Kawaguchi, K.; Saeki, Y.; Tanaka, K.; Wieland, T.; Graf, E.; Saeger, W.; Ronchi, C. L.; Allolio, B.; Buchfelder, M.; Strom, T. M.; Fassnacht, M.; Komada, M. Mutations in the Deubiquitinase Gene USP8 Cause Cushing's Disease. *Nat. Genet.* **2015**, *47* (1), 31−38.
(21) Centorrino, F.; Ballone, A.; Wolter, M.; Ottmann, C. Biophysical and Structural Insight into the USP8/14−3-3 Interaction. *FEBS Lett.* **2018**, *592* (7), 1211−1220.
(22) De Vries-van Leeuwen, I. J.; da Costa Pereira, D.; Flach, K. D.; Piersma, S. R.; Haase, C.; Bier, D.; Yalcin, Z.; Michalides, R.; Feenstra, K. A.; Jiménez, C. R.; de Greef, T. F. A.; Brunsveld, L.; Ottmann, C.; Zwart, W.; de Boer, A. H. Interaction of 14−3-3 Proteins with the Estrogen Receptor Alpha F Domain Provides a Drug Target Interface. *Proc. Natl. Acad. Sci. U. S. A.* **2013**, *110* (22), 8894−8899.
(23) Bozoky, Z.; Krzeminski, M.; Muhandiram, R.; Birtley, J. R.; Al-Zahrani, A.; Thomas, P. J.; Frizzell, R. A.; Ford, R. C.; Forman-Kay, J. D. Regulatory R Region of the CFTR Chloride Channel Is a Dynamic Integrator of Phospho-Dependent Intra- and Intermolecular Interactions. *Proc. Natl. Acad. Sci. U. S. A.* **2013**, *110* (47), E4427−4436.
(24) Stevers, L. M.; Lam, C. V.; Leysen, S. F. R.; Meijer, F. A.; van Scheppingen, D. S.; de Vries, R. M. J. M.; Carlile, G. W.; Milroy, L. G.; Thomas, D. Y.; Brunsveld, L.; Ottmann, C. Characterization and Small-Molecule Stabilization of the Multisite Tandem Binding between 14−3-3 and the R Domain of CFTR. *Proc. Natl. Acad. Sci. U. S. A.* **2016**, *113* (9), E1152−E1161.
(25) Sijbesma, E.; Hallenbeck, K. K.; Leysen, S.; de Vink, P. J.; Skóra, L.; Jahnke, W.; Brunsveld, L.; Arkin, M. R.; Ottmann, C. Site-Directed Fragment-Based Screening for the Discovery of Protein−Protein Interaction Stabilizers. *J. Am. Chem. Soc.* **2019**, *141* (8), 3524−3531.
(26) de Vink, P. J.; Andrei, S. A.; Higuchi, Y.; Ottmann, C.; Milroy, L.-G.; Brunsveld, L. Cooperativity Basis for Small-Molecule Stabilization of Protein-Protein Interactions. *Chem. Sci.* **2019**, *10* (10), 2869−2874.
(27) Wolter, M.; de Vink, P.; Neves, J. F.; Srdanovic, S.; Higuchi, Y.; Kato, N.; Wilson, A. J.; Landrieu, I.; Brunsveld, L.; Ottmann, C. Selectivity via Cooperativity: Preferential Stabilization of the P65/14−3-3 Interaction with Semi-Synthetic Natural Products. *J. Am. Chem. Soc.* **2020**, *142*, 11772.
(28) Andrei, S. A.; de Vink, P. J.; Sijbesma, E.; Han, L.; Brunsveld, L.; Kato, N.; Ottmann, C.; Higuchi, Y. Rationally Designed Semisynthetic Natural Product Analogues for Stabilization of 14−3-3 Protein-Protein Interactions. *Angew. Chem., Int. Ed.* **2018**, *57* (41), 13470−13474.

https://doi.org/10.1021/acsmedchemlett.1c00088
ACS Med. Chem. Lett. 2021, 12, 976−982